

Sustained Solar Fuel Production in Multiple Thermochemical Cycles Using Sol-Gel Derived Ferrite Nanopowders

R. Bhosale*¹, P. Sutar¹, A. Kumar¹, F. AlMamani¹, I. Alxneit², J.R. Scheffe³

¹Department of Chemical Engineering, College of Engineering, Qatar University, Doha, Qatar.

²Solar Technology Laboratory, Paul Scherrer Institute, 5232 Villigen PSI, Switzerland.

³Department of Mechanical and Aerospace Engineering, University of Florida, Gainesville, FL, USA.

rahul.bhosale@qu.edu.qa

ABSTRACT

In this paper, the sol-gel synthesis of Mg-doped Ni-ferrite i.e. Ni-Mg-ferrite was attempted by using propylene oxide (PO) as a proton scavenger. Effects of two important synthesis parameters such as amount of PO added during synthesis and aging time on physico-chemical properties such as phase composition, specific surface area (SSA), crystallite size, and particle morphology were studied by using different analytical methods such as powder X-ray diffractometer (PXRD), BET specific surface area analyzer, and scanning electron microscope (SEM).

Keywords: solar energy, thermochemical, hydrogen, water splitting, ferrite.

1 INTRODUCTION

Metal oxide (MO) based solar thermochemical H₂O and CO₂ splitting cycle is considered as one of the promising options for the production of solar H₂ or solar syngas. The H₂ produced can be directly utilized as a chemical fuel and the syngas can be reformed into liquid transportation fuels such as gasoline, diesel, kerosene, etc. via catalytic Fischer-Tropsch process.

MO based solar thermochemical splitting of H₂O and CO₂ process consists of two steps. In step 1, the MO is thermally reduced to lower valence MO or metal via solar thermochemical decomposition. On the other hand, in step 2, the reduced MO is regenerated by picking up oxygen from H₂O, CO₂, or a mixture of H₂O and CO₂, producing H₂, CO, or syngas.

In past, several kinds of MO systems have been examined towards solar thermochemical fuel production such as iron oxide cycle, zinc/zinc oxide cycle, tin/tin oxide cycle, mixed ferrite cycle, and ceria cycle [1-27]. Among these, researchers are recently targeting the ferrite materials such as Ni-ferrite, Co-ferrite, Sn-ferrite, Mn-ferrite, and etc. Among ferrites, the doped ferrites look very promising as due to the doping more chances of oxygen vacancy formation are possible and hence higher amounts of solar fuel production can be achieved. Hence, Ni-Zn-ferrite, Ni-Mn-ferrite, Ni-Sn-ferrite, and etc. are also studied in recent years. A typical ferrite based solar thermochemical cycle is presented in Figure 1.

In this study, attempts are made to synthesize a Mg doped Ni-ferrite (i.e. Ni-Mg-ferrite) by using propylene oxide (PO) assisted sol-gel method. The derived ferrite material was further characterized towards its phase and chemical composition, surface area (SSA), and microstructural morphology using various analytical methods such as powder x-ray diffraction (PXRD), BET surface area analyzer, and scanning electron microscope (SEM), respectively.

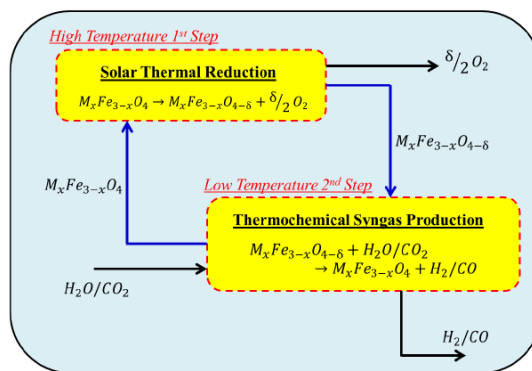


Figure 1. A typical ferrite based solar thermochemical H₂O and CO₂ splitting cycle.

2 EXPERIMENTAL

2.1 Materials

Precursors required for the sol-gel synthesis of Ni-Mg-ferrite i.e. nickel nitrate, magnesium nitrate, and iron nitrate were procured from Sigma Aldrich and Alfa Aesar. Likewise, the solvent ethanol and proton scavenger propylene oxide were also purchased from similar vendors. All the chemicals were used directly without any pre-treatment.

2.2 Sol-Gel Synthesis of Ni-Mg-ferrite

The sol-gel synthesis of Ni-Mg-ferrite were carried out at room temperature. At first, the metal nitrates were dissolved in the solvent ethanol with the help of sonic bath (with respective weight ratio). To this mixture of metal nitrates and ethanol, PO was added slowly as a proton scavenger and gel formation was achieved at room

temperature. After synthesizing the gel, it was aged for few hours (at room temperature). After aging, the gel was dried and the dried powder was further calcined at 800°C in presence of Air. The calcined powder was stored in a dry place and utilized towards the physico-chemical characterization. A typical, sol-gel route in case of Ni-Mg-ferrite is presented in Figure 2.

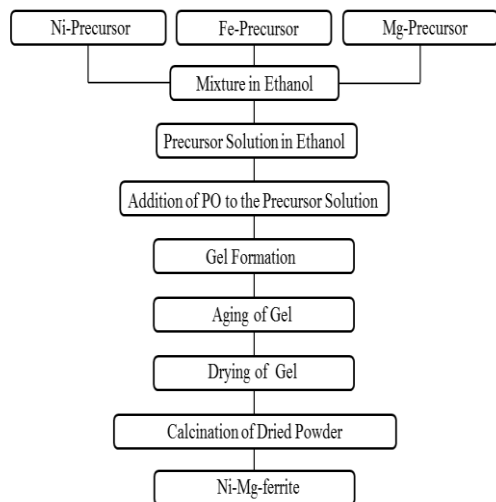


Figure 2. A typical sol-gel route for sol-gel synthesis of Ni-Mg-ferrite.

2.3 Physico-Chemical Characterization

Phase composition and crystallite size of the sol-gel derived Ni-Mg-ferrite was determined by using the Panalytical XPert MPD/DY636 powder X-ray diffractometer with CuK α radiation ($\lambda = 0.15418$ nm, voltage = 45 kV, current = 20 mA, angular range = 20 to 80° 2 θ , steps = 0.05° 2 θ , recording time = 5 s). Crystallite sizes were calculated by using the Scherrer's equation.

The SSA of the sol-gel derived Ni-Mg-ferrite was estimated using the BET surface area analyzer, ASAP 2420 from Micromeritics via the adsorption/desorption isotherms obtained after degassing the calcined Ni-Mg-ferrite powder at 200°C for 12 h.

The particle morphology and chemical composition of the sol-gel derived Ni-Mg-ferrite was analyzed with the help of a Zeiss Supra 55VP field-emission scanning electron microscope (SEM) equipped with a field emission gun and x-ray energy dispersive spectrometer (EDS) from Oxford Instruments. Ni-Mg-ferrite calcined powder was directly used for the SEM/EDS analysis without any coating by the conductive material. A secondary electron detector was used to probe the oxide layer topography with electron high tension (EHT) = 3 kV.

3 RESULTS AND DISCUSSION

To derive Ni-Mg-ferrite, 10 g of the metal nitrates of Ni, Mg, and Fe (with respective weight ratios) were dissolved in 20 ml of ethanol using sonic bath. To this mixture, different amounts of PO were added as proton scavenger and the gel formation was achieved. At first, the influence of amounts of PO on gel time, phase/chemical composition, crystallite size, and SSA of the sol-gel derived Ni-Mg-ferrite was tested.

As shown in Figure 3, as the amounts of PO added increases the time required for gel formation decreases. By adding 5 ml of PO, the Ni-Mg-ferrite gel formation can be achieved in 589 sec. As the amount increase upto 10 ml, the gel time decreases to 512 sec. Furthermore increase in the amount of PO added induces a quick Ni-Mg-ferrite gel formation. For instance, when 15 and 20 ml of PO was added the gel was formed in 444 and 330 sec, respectively. Addition of PO as a proton scavenger helps in freezing the molecular chains and reducing the time required for gel formation.

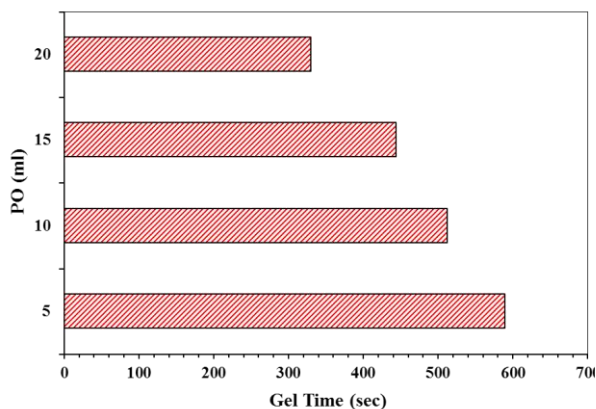


Figure 3. Effect of amount of PO added as a proton scavenger on gel time for Ni-Mg-ferrite.

Similar to the gel time, the effect of different amounts of PO added during sol-gel synthesis of Ni-Mg-ferrite on phase/chemical composition was also studied. The gels prepared with different amounts of PO were aged for 24 h, dried at 100°C for 1 h, and then calcined upto 800°C in air using muffle/box furnace. The calcined powder was further analyzed using PXRD and the obtained XRD patterns indicate no change in phase composition due to the usage of different amounts of PO. For instance, a sample PXRD pattern in case of Ni-Mg-ferrite prepared by using 20 ml of propylene oxide calcined at 800°C is shown in Figure 4. The EDS analysis also confirmed that the chemical composition of the derived Ni-Mg-ferrite remained unchanged even though different amounts of PO were used during synthesis.

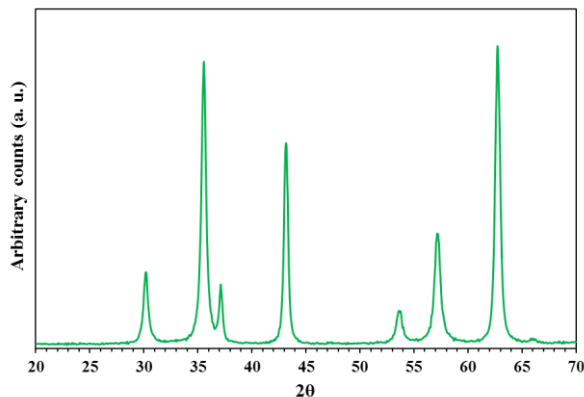


Figure 4. PXRD patterns for the sol-gel derived Ni-Mg-ferrite calcined at 800°C in air.

The PXRD patterns shown in Figure 4 indicate that the Ni-Mg-ferrite gel prepared by using 20 ml of PO and with 24 h aging calcined at 800°C in air for 1 h yields into a phase pure $\text{Ni}_{0.5}\text{Mg}_{0.5}\text{Fe}_2\text{O}_4$. Impurities of other metal oxides or pure metals are not seen in the PXRD patterns and hence it can be concluded that a phase pure composition of Ni-Mg-ferrite is achieved.

In addition to the phase composition, the effect of concentration of PO added during synthesis on crystallite size of the Ni-Mg-ferrite was explored and the obtained results are shown in Figure 5. The obtained results indicate that the crystallite size of the Ni-Mg-ferrite derived here does not get influenced due to the change in the concentration of propylen oxide. For instance, the crystallite size remain constant in the range of 39.55 to 40.12 nm even though the amounts of PO used changes from 5 to 20 ml.

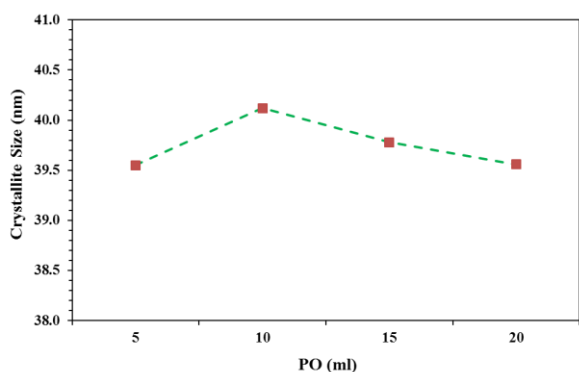
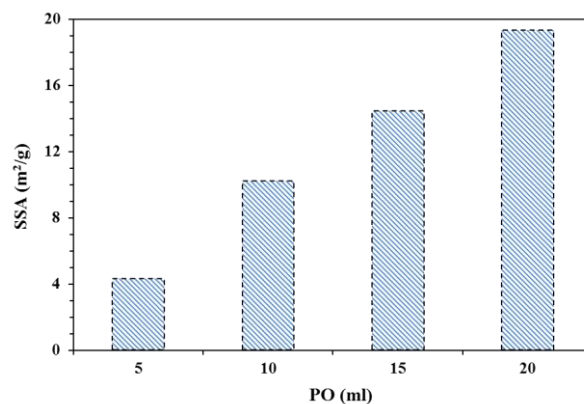


Figure 5. Effect of amount of PO added as a proton scavenger on crystallite size in case of Ni-Mg-ferrite.

After analyzing the effect of amounts of propylen oxide added on gel time, phase composition, and crystallite size, next we studied the effect of addition of PO on SSA.

The as-prepared gels with different amounts of PO (5 to 20 ml) were calcined in air up to 800°C and the calcined powder was further analyzed using BET surface area analyzer. The BET results are reported in Figure 6 which indicates significant increase in the SSA of the sol-gel derived Ni-Mg-ferrite due to the increase in the amounts of PO used during synthesis. When 5 ml of PO oxide was used, the SSA of Ni-Mg-ferrite was observed to be equal to 4.28 m²/g. However, when the amounts of PO increases to 10, 15 and 20 ml, the SSA also increases upto 10.23, 14.44, and 19.33 m²/g, respectively.

Figure 6. Effect of amount of PO added as a proton



scavenger on SSA of Ni-Mg-ferrite.

The sol-gel derived Ni-Mg-ferrite (calcined at 800°C) powder was further analyzed towards its powder morphology using scanning electron microscope (SEM). The images obtained (not shown here) indicate nanoparticle morphology with particle size in the range of 40 to 70 nm.

After studying the effect of addition of PO, next the effect of aging time on physico-chemical properties of sol-gel derived Ni-Mg-ferrite was also investigated. Aging improves the mechanical strength of the gel. During aging, the connectivity of the molecular network produced by the condensation reaction get better which finally results into significant homogeneity of the material synthesized. To examine the effect of aging time on physico-chemical properties of sol-gel derived Ni-Mg-ferrite, the gels prepared with PO = 20 ml were aged for 24 to 120 h at room temperature. After aging, gels were dried and further calcined at 800°C for 1 h in air. Calcined powders were characterized using PXRD, BET, and EDS to investigate the influence of aging time. The PXRD patterns confirm that the phase composition of the Ni-Mg-ferrite remains unchanged due to the alteration in the aging time. Furthermore, the SSA, porosity, and crystallite size of the was also remained constant irrespective of the increase in the aging time. These results indicate that, although aging helps to achieve the desired chemical homogeneity, other physico-chemical properties such as phase composition, SSA, porosity, and crystallite size stays intact.

4 CONCLUSIONS

The synthesis of Ni-Mg-ferrite nanoparticles was successfully achieved via PO assisted sol-gel method. Effect of PO as a proton scavenger and aging time on physico-chemical properties of sol-gel derived Ni-Mg-ferrite was investigated in detail. It was observed that with the increase in the amount of PO used during the sol-gel synthesis of Ni-Mg-ferrite, the time required for gel formation decreases. The phase composition and crystallite size of the sol-gel derived Ni-Mg-ferrite was observed to be unaffected due to the increase in the amount of PO used using synthesis. However, the SSA and pore volume was observed to be increased significantly. The study of effect of gel aging time shows that, although the chemical homogeneity can be increased via aging, the physico-chemical properties of Ni-Mg-ferrite remained unaltered.

ACKNOWLEDGEMENT

This publication was made possible by the NPRP grant (NPRP8-370-2-154) and UREP grant (UREP18-146-2-060) from the Qatar National Research Fund (a member of Qatar Foundation). The statements made herein are solely the responsibility of author(s). The authors also gratefully acknowledge the financial support provided by the Qatar University Internal Grant QUUG-CENG-CHE-14\15-10.

REFERENCES

- [1] S. Abanades, P. Charvin, and G. Flamant, *Chem. Eng. Sci.*, 62, 6323, 2007.
- [2] M. Chambon, S. Abanades, and G. Flamant, *AIChE J.*, 57, 2264, 2011.
- [3] M. Chambon, S. Abanades, and G. Flamant, *Int. J. Hydrogen Energy*, 34, 5326, 2009.
- [4] P. Loutzenhiser, M. Gálvez, I. Hischer, A. Stamatou, A. Frei, and A. Steinfeld, *Energy Fuels*, 23, 2832, 2009.
- [5] L. Schunk, W. Lipiński, and A. Steinfeld, *Chem. Eng. J.*, 150, 502, 2009.
- [6] A. Steinfeld, *Sol. Energy*, 78, 603, 2005.
- [7] W. Villasmil, M. Brkic, D. Wullemin, A. Meier, and A. Steinfeld, *J. Sol. Energy Eng.* 136, 011016, 2014.
- [8] D. Dardor, R.R. Bhosale, S. Gharbia, A. Kumar, and F. Al Momani, *Journal of Emerging Trends in Engineering and Applied Sciences*, 6, 129, 2015.
- [9] D. Dardor, R. Bhosale, S. Gharbia, A. AlNouss, A. Kumar, and F. AlMomani, *International Journal of Engineering Research & Applications*, 5, 134, 2015.
- [10] R.R. Bhosale, A. Kumar, van den Broeke, Leo JP, S. Gharbia, D. Dardor, M. Jilani, J. Folady, M.S. Al-Fakih, and M.A. Tarsad, *Int J Hydrogen Energy*, 40, 1639, 2015.
- [11] J.R. Scheffe, A. Francés, D.M. King, X. Liang, B.A. Branch, A.S. Cavanagh, S.M. George, and A.W. Weimer, *Thin Solid Films*, 517, 1874, 2009.
- [12] R.R. Bhosale, R.V. Shende, and J.A. Puszynski, *Int J Hydrogen Energy*, 37, 2924, 2012.
- [13] R. R. Bhosale, R. Khadka, J. Puszynski, R. Shende, J. Renewable Sustainable Energy, 3, 063104, 2011.
- [14] J.R. Scheffe, M.D. Allendorf, E.N. Coker, B.W. Jacobs, A.H. McDaniel, and A.W. Weimer, *Chem. Mater.*, 23, 2030, 2011.
- [15] R. R Bhosale, A. Kumar, F. AlMomani, U. Ghosh, D. Dardor, Z. Bouabidi, M. Ali, S. Yousefi, A. AlNouss, M. S. Anis, M. H. Usmani, M. H Ali, R. S Azzam, A. Banu, *Energy Convers. Manage.*, 112, 413, 2016.
- [16] J.R. Scheffe, R. Jacot, G.R. Patzke, and A. Steinfeld, *J. Phys. Chem. C*, 117, 24104, 2013.
- [17] R. R Bhosale, A. Kumar, F. AlMomani, and I. Alxneit, *Ceram. Int.*, 42, 2431, 2016.
- [18] J.R. Scheffe, A.H. McDaniel, M.D. Allendorf, and A.W. Weimer, *Energy Environ. Sci.*, 6, 963, 2013.
- [19] R. R Bhosale, A. Kumar, F. AlMomani, and I. Alxneit, *Ceram. Int.*, 42, 6728, 2016.
- [20] J.R. Scheffe, J. Li, and A.W. Weimer, *Int J Hydrogen Energy*, 35, 3333, 2010.
- [21] R. R Bhosale, A. Kumar, F. AlMomani, U. Ghosh, S. Al-Muhtaseb, R. Gupta, and I. Alxneit, *Ceram. Int.*, 2016 (Accepted – In Press).
- [22] M. Neises, M. Roeb, M. Schmücker, C. Sattler, and R. Pitz-Paal, *Int. J. Energy Res.*, 34, 651, 2010.
- [23] R.R. Bhosale, R.V. Shende, and J.A. Puszynski, *Journal of Energy and Power Engineering*, 4, 27, 2010.
- [24] R.R. Bhosale, R.V. Shende, and J.A. Puszynski, *Int. Rec. Chem. Eng.*, 2, 852, 2010.
- [25] V. Amar, J. Puszynski, and R. Shende, *J. Renewable Sustainable Energy*, 7, 023113, 2015.
- [26] R.R. Bhosale, R.V. Shende, and J.A. Puszynski, *MRS Proceedings*, mrsf11-1387-e09-07 (2012)
- [27] R.R. Bhosale, I. Alxneit, van den Broeke, Leo LP, A. Kumar, M. Jilani, S.S. Gharbia, J. Folady, and D. Dardor, *MRS Proceedings*, mrs14-1675-rr06-10 (2014).